Progress In Electromagnetics Research B, Vol. 55, 347–364, 2013

A PASSIVE WIRELESS GAS SENSOR BASED ON MICROSTRIP ANTENNA WITH COPPER NANORODS

Taha A. Elwi[1, *] and Wisam J. Khudhayer[2]

[1]Department of Communication Engineering, Al-Mamon University College, Baghdad, Iraq

[2]Electrochemical Engineering Department, University of Babylon, Babylon, Iraq

Abstract—Applications of copper (Cu) nanorod arrays, produced by glancing angle deposition (GLAD) technique, which extends the function of conventional microstrip antennas to encompass passive wireless gas sensors at microwave frequencies are presented. The proposed microstrip antenna consists of Cu nanorod arrays grown on silicon wafers which were coated with thin films of Cu of 50 nm in thickness. To study the effect of the length of Cu nanorods on antenna performance, Cu nanorods of different lengths (400, 700, and 1000 nm) were fabricated. The effects of Cu nanorods morphologies (Cu thin film, closely-spaced Cu nanorods, and well-separated Cu nanorods), were investigated too. Conventional microstrip antennas based on sputtered Cu thin film were prepared for comparison. It was found that as the length of Cu nanorods increases, the antennas exhibit a wider bandwidth and lower frequency resonance than those of the conventional antennas based on Cu thin film. Furthermore, moving from flat surface to well-separated nanorods results in a decrease in the resonant frequency, while there was no observable effect on the bandwidth. These enhancements are attributed to the mutual coupling occurring among Cu nanorods. Based on the antenna characterization, the 1000 nm long Cu nanorods sample was selected for gas detection measurements due to its observed sharp resonance and narrow bandwidth. The detection mechanism is based on the change of in the magnitude of the reflection coefficient as well as the resonant frequency due to the introductions of different gases. The proposed sensor based on Cu nanorods shows a significant response in

Received 20 August 2013, Accepted 16 October 2013, Scheduled 18 October 2013

* Corresponding author: Taha A. Elwi (taelwi@ualr.edu).

response to the introduction of different gases such as oxygen, nitrogen, and nitrogen, while the conventional antenna shows no measurable response. It is believed that the proposed sensor is applicable to the other gases based on the suggested sensing mechanism.

1. INTRODUCTION

Copper has been applied in several branches of industries due to its favorable electrical properties [1]. For example, bulk Cu is widely used in the fabrication of microstrip antennas due to the inherent need of conductive parts such as patches and ground planes [2]. Recently, sputter-deposited metallic nanorods produced by glancing angle deposition (GLAD) technique have shown great promise in different applications such us heat transfer [3] and energy applications [4] due to their unique physical and chemical properties such as single-crystal property and formation of uncommon crystal planes [4]. However, their application in antennas has not been explored yet. GLAD nanorods can be grown with high aspect ratios, which can lead to high impedance values of an individual nanorod. Moreover, length of the GLAD nanorod can be controlled to range from some hundreds to few thousands of subwavelengths at the microwave regime [5].

On the other hand, wireless gas detection has received a substantial attention by researchers due to the recent demands in many industrial, medical, and commercial applications [6]. Therefore, there are several attempts for constructing gas detectors based on various nanoscale structures and organic materials [6]. Nanoscale structures became one of the frontiers that can support the new generations of antenna technology. For example, the change in the electrical response of the multi walled carbon nanotube films due to the presence of different gases at room temperature has been recently investigated by Sidek et al. [7]. The Radio Frequency IDentification (RFID)-enabled wireless gas sensor was used to detect different gases such as ammonia, methanol, ethanol, acetone, and nitrogen oxide by integrating conformal RFID antenna to carbon nanotube films in a chipless fashion [8]. Balachandran et al. [9] developed a capacitive sensor for ethylene gas detection by integrating tin oxide (SnO_2) nanoparticles to a microstrip antenna. Furthermore, functionalized carbon nanotubes and polymethylmethacrylate were embedded in composite polymer thin films to design passive wireless detectors for detecting hazard biological materials and vapors [10]. In another study [11], vertically aligned multi walled carbon nanotube arrays were investigated for ammonia sensing at microwave frequencies. The

carbon nanotubes-based gas sensors were developed to detect different gases based on the change in the reflection coefficient magnitude as a response to the introduction of each gas [12, 13]. A one-dimensional hydrogen detector based on an individual zinc oxide (ZnO) nanorod was developed and investigated for its gas detection property [14]. Highly crystalline tungsten oxide nanorods were grown onto a silicon substrate and used as a temperature-dependent gas sensor operated within the temperature range of 20–250°C [15]. J. X. Wang et al. [16] fabricated a hydrogen gas detector which comprised from vertically aligned ZnO nanorod arrays grown on ZnO thin film. In addition, a gas sensor based on multi walled carbon nanotube-silicon dioxide composite layer deposited on a planar inductor-capacitor resonant circuit connected to a loop antenna was studied for monitoring carbon dioxide, oxygen, and ammonia [17]. Other examples of nanostructured gas detectors reported in the literature [18–20] were operated by measuring the impedance of coated capacitors with a gas-responsive polymers mixed with carbon nanotubes or ceramic such as hetero polysiloxane.

Most of the previously reported gas sensors/detectors suffer from several common problems such as wiring connections between the sensor head, power supply, and data processing circuitry [6]. In addition, the integration of these sensors/detectors with wireless devices is very difficult due to antenna matching limitations. Moreover, gas sensors/detectors based on carbon nanotubes depend on the carbon nanotubes functionalization with the environmental gases which is difficult to control [20]. Nevertheless, gas sensors based on gas-responsive polymers or ceramic materials suffer from limited battery lifetime [15]. Due to these limitations, there exists a great interest in developing novel gas sensors/detectors based on metallic nanostructures without the need for wiring connections or chemical fictionalization. The sensor should be easy to integrate with wireless devices to alleviate issues pertaining battery life time. Finally, in all pervious researches, the sensing process is based on the chemical and/or physical interactions between the gas particles and materials due to gas contaminations. However, in our proposed senor, the sensing philosophy is based on the electromagnetic fields interactions between the gas particles and the trapped fields among Cu nanorods.

The objective of this study is to extend the function of conventional microstrip antennas to include wireless gas detection based on measuring the change in the reflection coefficient and resonant frequency upon exposure to different gases under the atmospheric pressure.

The proposed sensor was constructed from a silicon substrate

backed with a Cu plate which functions as the ground plane for the microstrip antenna. The microstrip antenna patch was loaded with 2-D arrays of Cu nanorods and is fed a 50 Ω microstrip transmission line connected to a 50 Ω Sub Miniature version A (SMA) connector. Six different prototypes of microstrip antennas based on different lengths and separations of the Cu nanorod arrays were tested. The first prototype was fabricated based on conventional bulk Cu, the second is from sputtered Cu thin film, and the rest were fabricated from Cu nanorods with different lengths and morphologies/separations. The Cu nanorods based antenna that achieved the best response for gas detection was compared to the conventional antenna based on bulk Cu.

The Cu nanorods were fabricated using GLAD technique which provides the capability for growing nanostructure arrays with enhanced material properties such as high electrical/thermal conductivity and reduced oxidation compared to the polycrystalline films [21]. It offers simple, single-step, cost- and time-efficient method to fabricate nanostructured arrays of various elemental materials as well as alloys and oxides. The GLAD technique uses the "shadowing effect," through which obliquely incident atoms/molecules can only deposit on the tops of higher surface points, such as to the tips of a nanostructured array or on the highest points of a rough or patterned substrate. Some rods grow faster in the vertical direction due to the statistical fluctuations in the growth and effect of initial substrate surface roughness. These rods capture the incident particles due to their higher height, while the shorter rods get shadowed and cannot grow anymore. As a result, isolated nanostructures can be formed. The deposition rate, incidence angle, substrate rotation speed, working gas pressure, substrate temperature, and the initial surface topography of the substrate can be utilized to control the shadowing effect.

2. ANTENNA AND SENSOR FABRICATION

The schematic of the GLAD experimental setup (Excel Instrument, India) was used in the present study as shown in Fig. 1. In our experiments, we employed the DC magnetron sputter technique for the fabrication of the vertically aligned Cu nanorod arrays and flat Cu film coatings using a 99.9% pure Cu source (target) and 7.6 cm in diameter. The substrate was mounted on a sample holder located at a distance of about 12 cm from the source. During the growth, the substrate was tilted so that the deposition angle θ, measured from the substrate normal, is adjusted to the desired value. The substrate was attached to a stepper motor and rotates around its normal axis at a speed of 2 rpm

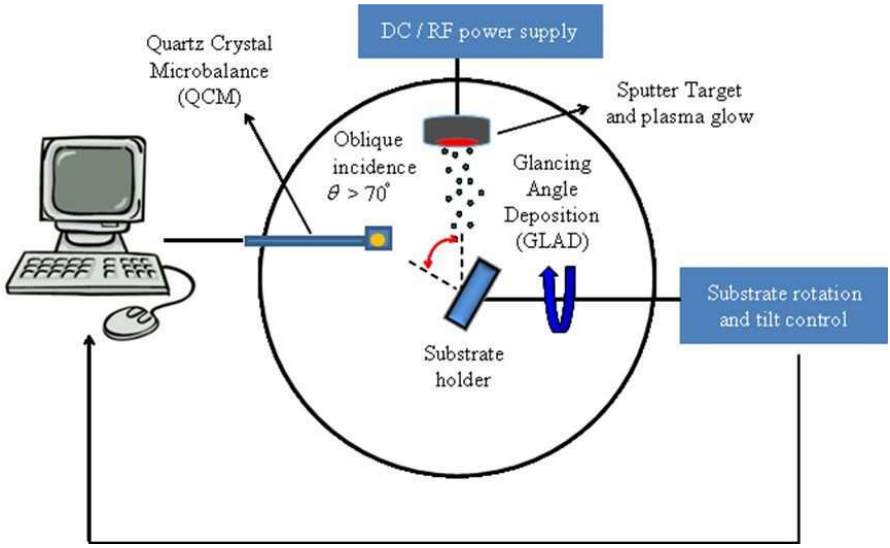

Figure 1. A schematic of GLAD technique used for the fabrication of Cu nanorod arrays.

for growing vertical Cu nanorods. The depositions were performed under a base pressure of 5×10^{-7} Torr using a turbo-molecular pump backed by a mechanical pump. Sputter plasma was generated using a DC power value of 200 W and an ultra pure Argon flow with working gas pressure of 2.5 mTorr. Analysis based on cross sectional scanning electron microscopy (SEM, FESEM-6330F, JEOL Ltd, Tokyo, Japan) images shows that the growth rates of Cu coatings are 25, 10, and 8.6 nm/min for deposition angles of 0° (flat film), 80° (closely-spaced nanorods), and 87° (well-separated nanorods), respectively. Nanorods with different lengths (L) are grown by changing the deposition time. The depositions are performed on a $2 \times 2\,\text{cm}^2$ silicon wafer substrates. Before depositing the Cu nanorods, silicon substrates are coated with a flat 50 nm thick Cu film layer that are deposited at normal incidence which was used as a conductive layer.

The well-separated Cu nanorods were grown at lengths $L = 400$, 700, 1000 nm and were labelled as samples I, II, and III, respectively. A closely-spaced Cu nanorods deposited at 80° was named as sample IV, and the flat Cu thin film that was deposited at normal incidence as sample V. Finally, the reference sample based on bulk Cu was denoted by sample VI.

Figure 2 depicts the wireless passive gas sensor comprised of Cu nanorods deposited on a Cu film coated silicon substrate ($\varepsilon_r = 11.9$

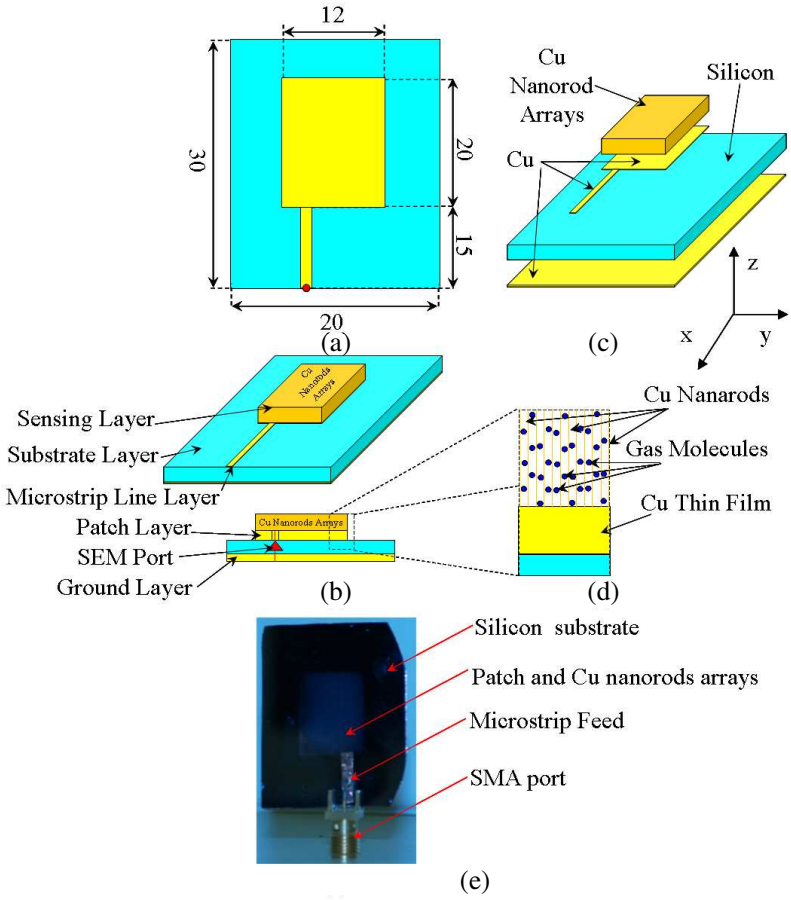

Figure 2. The proposed sensor, (a) the front view, (b) the 3-D view, (c) de-assembled view and (d) zoomed out view of the Cu nanorods on top of Cu thin film. Note: The geometry (a)–(d) is not to scale. The presented dimensions are in mm.

and $\tan\delta = 0.01$) and stacked on FR4 substrate. The rectangular patch was backed by Cu ground plane. The FR4 substrate was used to reinforce the silicon substrate, which is a fragile wafer, using polyimide glue of $\varepsilon_r = 1.05$ and $\tan\delta = 0.1$. Due to the significant difference between the sizes of the Cu nanorods and the rest components of the sensor, it is neither possible nor practical to simulate the Cu nanorods based sensor.

When the microstrip antenna based on Cu nanorods arrays is exposed to any gas, the effective complex relative permittivity, ε'_r

and ε_r'', of the space between the Cu nanorods varies with the gas introduction which changes the effective permittivity of the sorted medium among the Cu nanorods as described in the conceptual diagram in Fig. 3(a). This change may be reflected on the antenna performance due to the change on the surface waves and currents on the patch of the antenna; that can be detected as sensing action due to the gas introduction. To test this hypothesis, an experimental setup is used for demonstrating the gas detecting operation. The sensor was placed inside a chamber (foam box) and the gas runs through pipes into the chamber. A hole on the top of the chamber exhausts the gas so that the chamber pressure is kept at the atmospheric pressure. The foam box dimensions in height $\times$ width $\times$ length are $70 \times 60 \times 100\,\text{cm}^3$, respectively. Agilent E5071B, 300 kHz–8.5 GHz ENA series Network Analyzer and SN05499505 coaxial cable were used to measure the frequency spectrum of the reflection coefficient (S_{11}), the only measured response for sensing action, at the SMA terminal. The gas flow rates were controlled utilizing a mass-flow controller as schematically depicted in Fig. 3(b). A stop watch was used for recording the saturation time at which the detector does not response for the gas introduction any more. The settling time that was required by the sensor to return back to its original state, before the gas introduction, was monitored too. The S_{11} spectra were measured before and after gas introductions into the chamber to realize the difference in the resonant frequency, which corresponds to the presence of the introduced gas.

3. RESULTS AND DISCUSSION

In this section, first SEM was utilized to study the morphology of the GLAD Cu nanorods. Then, an experimental comparison between the performance of the proposed microstrip antenna based on Cu nanorods and the conventional one was performed. Finally, the sensor performance based on Cu nanorods was evaluated and compared with that of the reference sample. The measurements for the antenna and sensor characterizations were performed utilizing network analyzer and anechoic chamber instruments.

3.1. Morphology of GLAD Cu Nanorods

Arrays of Cu nanorods with different lengths and morphologies were fabricated to systematically study the effect of the nanorods length (L) and separation (S) on the performance of the antenna/gas sensor. The SEM was used to investigate the morphology of the deposited Cu

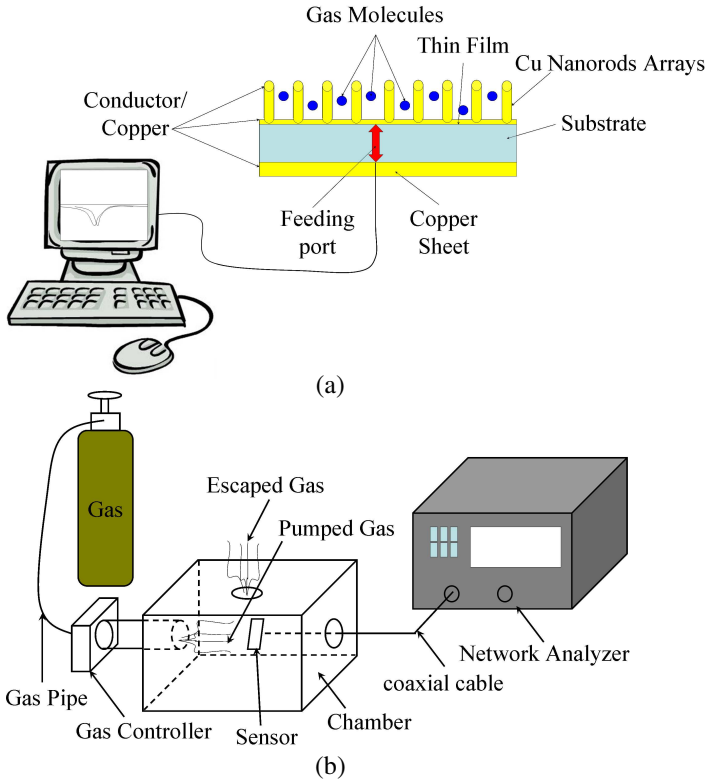

Figure 3. Detection process. (a) Conceptual presentation of gas detection and (b) Experimental setup used for gas detecting test. Note: The presented geometry in this figure is not scalable.

nanorods. The top and cross sectional SEM views of conventional flat Cu thin film deposited at normal incidence, closely-spaced Cu nanorods deposited at 80°, and isolated Cu nanorods of lengths 400, 700, and 1000 nm deposited at 87° are shown in Figs. 4(a)–(e). The SEM images show that Cu nanorods of different lengths, Figs. 4(c)–(e), have an isolated columnar morphology, while closely spaced Cu nanorods are relatively smoother, Fig. 4(b), and conventional Cu film has a very smooth surface, Fig. 4(a). At early stages of GLAD growth, the number density of the Cu nanorods is larger, and they have diameters as small as 5–10 nm. As they grow longer and some of the rods stop growing, due to the shadowing effect, their diameter grows up to 100 nm. The average gap among the Cu nanorods also changes with their length from 5–10 nm up to 50–100 nm at later

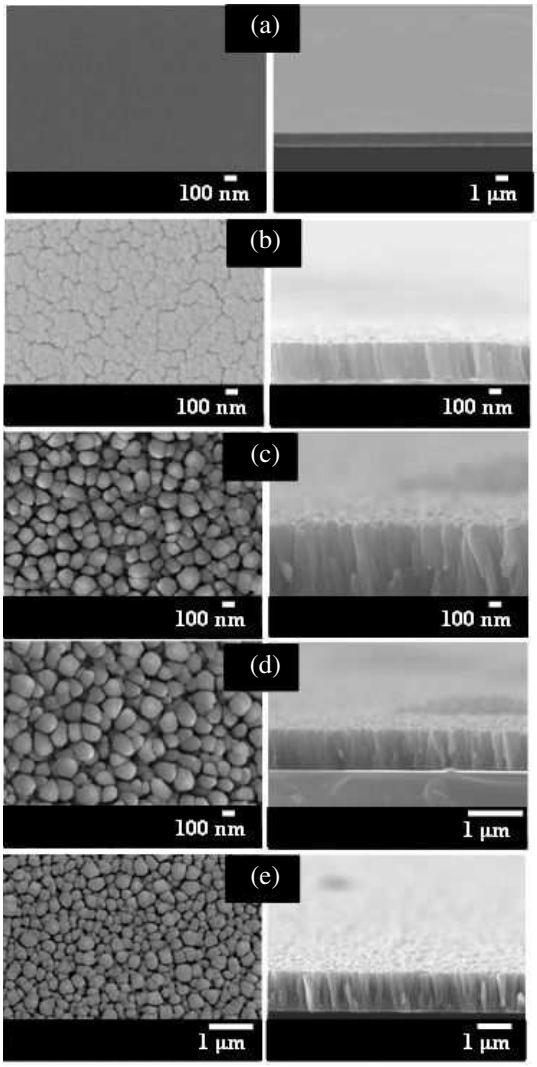

Figure 4. Left side SEM images show the top views and the SEM images on the right side represent the cross-sectional views of: (a) sample I, (b) sample II (c) sample III, (d) sample IV, and (e) sample V.

stages. As can be seen from Figs. 4(c) and (e), the top of the vertical columns has a pyramidal shape with four facets, which indicates that an individual column might have a single crystal structure and needs further crystal structure analysis. This observation is consistent with

previous studies [21] as well as our recent study [4] which reported that individual metallic nanorods fabricated by GLAD are typically single crystal. Single crystal rods do not have any interior grain boundaries and have faceted sharp tips. This property allows for reduced surface oxidation which can greatly increase the electrical conductivity, resistance to oxidation-degradation, and therefore robustness of the Cu nanorods.

3.2. Antenna Performance

The conventional microstrip antenna, (reference sample VI), was characterized theoretically and experimentally as illustrated in Figs. 2(a) and (b). The commercial software package CST Micro Wave

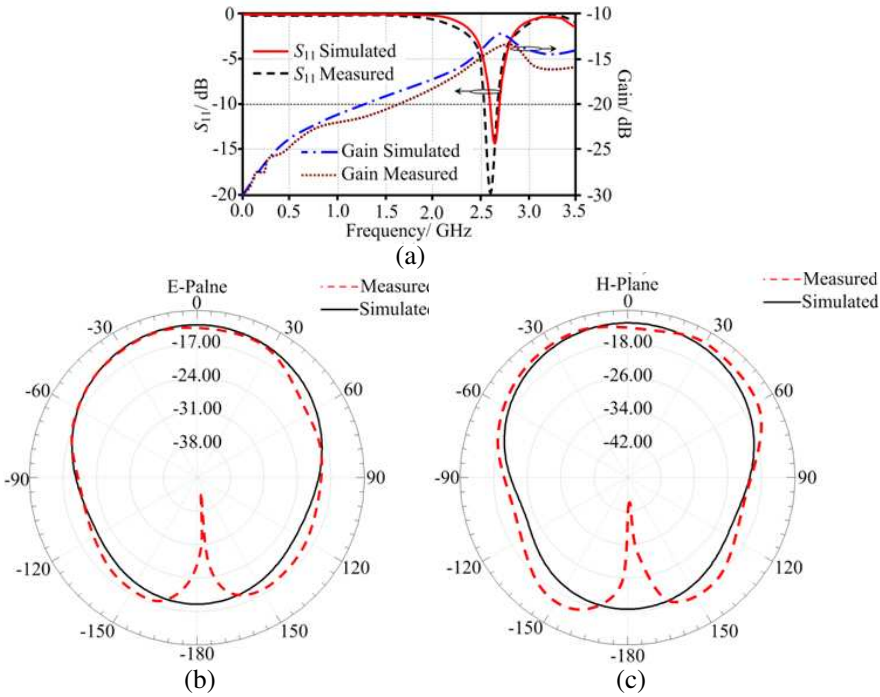

Figure 5. Measured and simulated results of, (a) S_{11} and boresight gain spectra, (b) the polar cut of the radiation pattern at $\Phi = 0°$ in the E (y-z) plane and (c) the polar cut of the radiation pattern at $\Phi = 90°$ in the H (x-z) plane for the conventional Cu microstrip antenna (sample #VI). Note: The measured radiation patterns are at 2.6 GHz.

Studio (MWS), which is based on the FIT technique, was utilized for characterizing the performance of the conventional antenna [22]. The measured and simulated frequency spectra of S_{11} and boresight gain spectra of the conventional microstrip antenna are presented in Fig. 5. It was found that the simulated results of the conventional antenna are in a good agreement with the measured results. The conventional antenna exhibits -10 dB return loss bandwidth of 1.8% and $S_{11} = -20$ dB at 2.61 GHz with the boresight gain of about -15 dBi as shown in Fig. 5(a). Figs. 5(b) and (c) show the measured and simulated radiation patterns for sample VI. A good agreement was observed between simulated and measured results as depicted in Fig. 5.

Next, the measurements of S_{11} spectra for the microstrip antennas with Cu nanorod arrays were compared to that of the conventional microstrip antenna. This comparison helps to clarify the effects of introducing Cu nanorods arrays on the performance of the microstrip antenna. Nevertheless, for gas detection tests, the prototype that provides the best matching with the lowest frequency resonance was chosen.

We experimentally studied the effects of L and S of the Cu nanorods on the performance of the microstrip antenna. Six prototypes were constructed using sputtered Cu thin film (sample V), closely-spaced Cu nanorods (sample IV), and isolated Cu nanorods of different

Table 1. Performance of the fabricated prototypes.

Sample Number	L (nm)	Sample name	S_{11} magnitude (dB)	Resonant Frequency (GHz)	Bandwidth (GHz)
I	400	Isolated Cu nanorods	-21	2.15	1.00
II	700	Isolated Cu nanorods	-15	1.50	0.75
III	1000	Isolated Cu nanorods	-50	1.51	0.35
IV	1000	Closely-spaced Cu nanorods	-25	1.80	0.50
V	1000	Flat Cu thin film	-23	2.50	0.65
VI	---	Bulk Cu (Reference)	-20	2.61	0.21

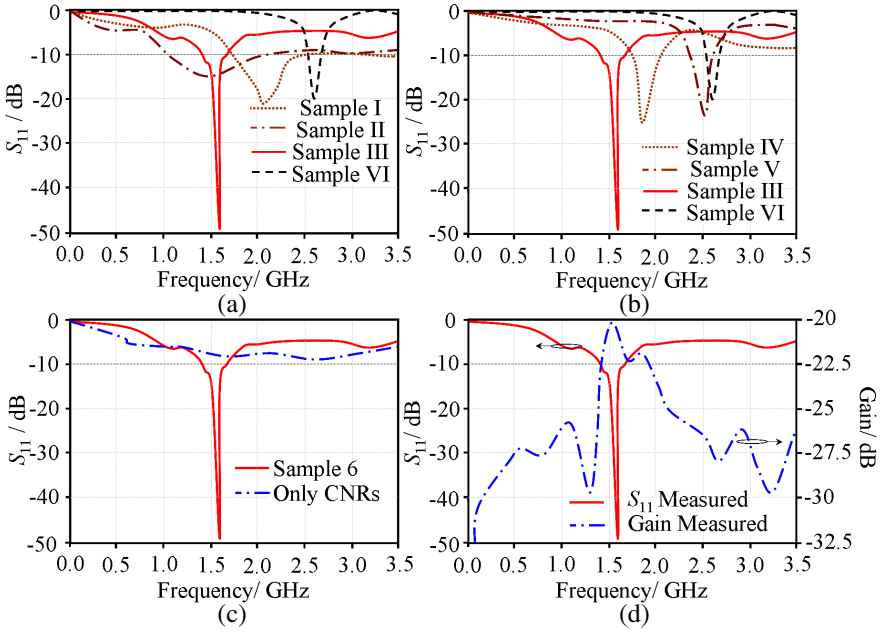

Figure 6. Measured S_{11} and boresight gain spectra of the CNRs based and conventional microstrip antenna samples for, (a) and (b) the effects of CNRs length and nanostructure morphology on S_{11} spectra, (c) the effect of introducing the underlying 50 nm thin film of Cu below the CNRs on the S_{11} spectra, and (d) the S_{11} and boresight gain spectra of sample III.

lengths. The measured magnitude of S_{11}, resonant frequency, and bandwidth of these samples are listed in Table 1 and compared with sample VI as shown in Figs. 6(a) and (b). From the results shown in Fig. 6(a), it was found that as L of Cu nanorods increases, the antenna exhibits wider bandwidth and lower resonant frequency in comparison to the conventional antenna. This enhancement is believed to be due to the mutual coupling occurring among Cu nanorods that creates subwavelength resonance due to the plasmonic effects of the Cu nanorods and the chirality of such complex medium [23]. Fig. 6(b) shows that as the morphology of the antenna is changed from a flat surface to closely-spaced nanorods, and then to isolated nanorods, the resonant frequency decreases. On the other hand, there is no observable effect of the Cu nanorods separation on the bandwidth. In addition, comparison of the measured S_{11} spectra for the sample III and another similar antenna but this time without the underlying

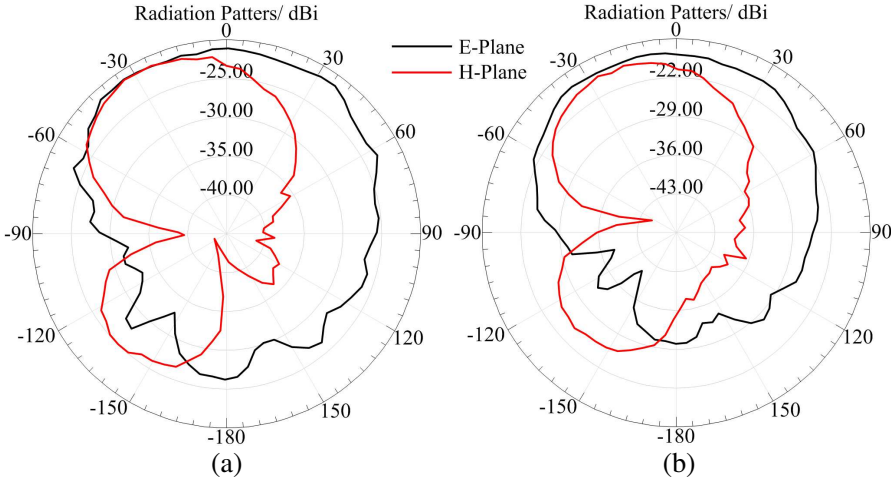

Figure 7. Measured radiation patterns at 2.3 GHz of two similar Cu nanorod-based antennas of sample III at $\Phi = 0^\circ$ in the E (y-z) and at $\Phi = 90^\circ$ in the H (x-z) plane, (a) for the first prototype and (b) the second prototype.

50 nm thick Cu thin film is presented in Fig. 6(c). The results reveal the necessity of using a conducting thin film in order to provide a coupling among Cu nanorod arrays. Fig. 6(d) shows the boresight gain versus frequency of sample III. The peak gain of the Cu nanorods antenna is about -20 dBi at 1.51 GHz. Comparing with results in Figs. 6(a) and 6(b), it was observed that the microstrip antenna with 1000 nm long Cu nanorods exhibits the best matching at lost frequency resonance and the best defined peak below -20 dB, which can be utilized for the highly sensitive and accurate gas detection measurements.

In Fig. 7, the radiation patterns at $\Phi = 0^\circ$ and 90° are shown at 2.3 GHz. It was found that the gains of sample III are -20.3 and -20.9 dBi at $\Phi = 0^\circ$ and 90°, respectively. Radiation pattern measurements were also reported for a second prototype of sample III for verification purposes. The radiation patterns presented in Fig. 7 are significantly different than those of sample VI as shown in Figs. 5(b) and (c). These differences clearly show the effect of Cu nanorods when incorporated into the microstrip antenna structure.

3.3. Characterization of Gas Detection

The detection capability of the proposed wireless sensor of sample III is based on the interaction between the induced waves on the Cu

nanorod arrays with the surrounding environment. The proposed senor is applicable for detection of any type of gas under the atmospheric pressure based on the sensing mechanism explained above. However, for the demonstration purpose, the gas sensing was performed on three different gases oxygen, argon, and nitrogen. The detector response is based on measuring the change in S_{11} spectra which corresponds to the introduced gases. The experimental setup consists of a chamber in which the sensor was attached to sidewall to avoid any vibration during the measurements. The Agilent network analyzer model E5071B with

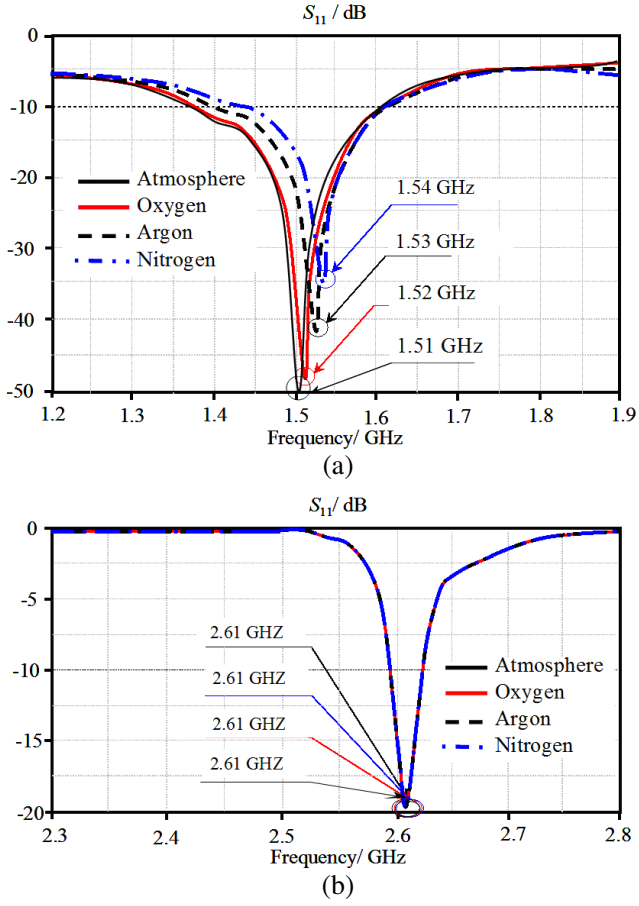

Figure 8. Measured S_{11} spectra in three different gases (oxygen, argon and nitrogen) with respect to the atmosphere. (a) Sample III: Microstrip antenna with 1000 nm long CNR arrays and (b) Sample IV: Conventional bulk Cu microstrip antenna as reference.

frequency accuracy, $+/-5$ ppm, and trace noise, 0.001 dB rms, was utilized to monitor the spectrum of S_{11} magnitude.

The microstrip antenna of sample III was chosen for gas detection tests due its excellent matching. The reference sample VI was also used for comparison in an effort to show the difference in the antenna response to the gas introduction. In each test, the antenna was exposed to one of the three different gasses in a controlled ambient atmosphere. The performance was measured in terms of S_{11} after the gas introduction and the results are presented in Fig. 8. The resonant frequency and S_{11} of sample III significantly changed due to the introduction of each individual gas as shown in Fig. 8(a). These changes were observed after a relatively short time of about 30 seconds from the gas introduction and for a slow gas flow rate of about 1000 ml/min. The resonant frequency was reduced after introducing oxygen gas by 10 MHz, while it is shifted by 20 and 30 MHz for argon and nitrogen gases, respectively. Moreover, the return loss magnitude was decreased from -50 to -47, -42, and -38 dB after exposing the antenna to oxygen, argon, and nitrogen gases, respectively. Similar measurements were carried out on sample VI. It was found that there is no measurable change in S_{11} or resonant frequency in response to the introduction of the different gases as shown in Fig. 8(b). The details of gas type, the saturation time, settling time, and flow rates are listed in Table 2 for both samples III and IV.

Table 2. Saturation and settling time with different gases.

Sample Number	Gas type	Saturation time	Settling time	Flow rate (ml/min)
III	Oxygen	30 sec.	33 sec.	1000
	Argon	25 sec.	36 sec.	1000
	Nitrogen	28 sec.	34 sec.	1000
VI	Oxygen	---	---	1000
	Argon	---	---	1000
	Nitrogen	---	---	1000

4. CONCLUSION

A novel wireless gas sensor utilizing Cu nanorods operating at the microwave frequency region was demonstrated. The proposed sensor is composed of Cu nanorod arrays grown by GLAD technique on a conventional microstrip antenna to distinguish different gases at the

atmospheric pressure. The performance of the sensor was tested and compared to an antenna sample without Cu nanorods. Bandwidth of the microstrip antenna with Cu nanorods of 1000 nm length is 0.35 GHz which is higher than that of the conventional bulk Cu microstrip antenna, which is 0.21 GHz. Moreover, the Cu nanorods based microstrip antenna exhibits a resonant frequency of 1.51 GHz which is lower than the 2.61 GHz value for the conventional microstrip antenna, resulting in an increase in the miniaturization factor for the microstrip antenna based Cu nanorods. However, the measured gain is about -20.3 dBi which is lower than -15 dBi for the conventional antenna. Furthermore, an experimental study has been performed to test the antenna return loss spectra for Cu nanorods with different lengths and separations. It was found that the bandwidth of the Cu nanorod arrays antenna increases with the length of Cu nanorods. As the Cu coating morphology was changed from flat surface to closely-spaced nanorods, and then to isolated Cu nanorod arrays, a reduction in the resonant frequency has been observed without a notable effect on the bandwidth. Finally, the microstrip antenna patch with 1000 nm long CNu nanorods was selected for gas detection studies due to the sharp and well defined peak at -50 dB where its bandwidth becomes very narrow, especially after -20 dB. Gas detection measurements, under the atmospheric pressure, on Cu nanorods antenna samples revealed a shift in the resonance frequency by 10 MHz, 20 MHz, and 30 MHz in response to the introduction of oxygen, argon, and nitrogen, respectively, while the conventional microstrip antenna shows no response. More in depth theoretical investigation is required for better understanding of the unusual behavior of the proposed microstrip antenna/gas detector based on Cu nanorods.

ACKNOWLEDGMENT

The authors would like to thank the UALR Nanotechnology Center and Dr. Fumiya Watanabe for his valuable support and discussions during SEM measurements. Finally, the authors appreciate Department of System Engineering and Department of Applied Science at UALR for their valuable support during the numerical simulation and experimental work.

REFERENCES

1. Kelsall, R., I. W. Hamley, and M. Geoghegan, *Nanoscale Science and Technology*, John Wiley & Sons, Ltd., The Atrium, Sothern Gate, Chichester, England, Apr. 2005.

2. Burke, P. J., S. Li, and Z. Yu, "Quantitative theory of nanowire and nanotube antenna performance," *IEEE Transactions on Nanotechnology*, Vol. 5, No. 4, 314–334, Jul. 2006.
3. Sesen, M., W. Khudhayer, T. Karabacak, and A. Kosar, "Compact nanostructure integrated pool boiler for microscale cooling applications," *Micro & Nano Letters*, Vol. 5, No. 4, 203–206, May 2010.
4. Khudhayer, W. J., N. Kariuki, X. Wang, D. J. Myers, A. U. Shaikh, and T. Karabacak, "Oxygen reduction reaction electrocatalytic activity of glancing angle deposited Pt nanorod arrays," *Journal of Electrochemical Society*, Vol. 158, No. 8, B1029–B1041, 2011.
5. Ventra, M., S. Evoy, and J. R. Heflin, "Introduction to nanoscale science and technology," *Spring Science & Businesses Media, Inc.*, Spring Street, New York, Mar. 2004.
6. Wilson, J. S., *Sensor Technology Handbook*, Vol. 1, Elsevier, Oxford, England, Dec. 2004.
7. Sidek, R. M., F. A. M. Yusof, F. M. Yasin, R. Wagiran, and F. Ahmadun, "Electrical response of multi-walled carbon nanotubes to ammonia and carbon dioxide," *IEEE International Conference on Semiconductor Electronics (ICSE)*, Vol. 4, No. 22, 263–266, Aug. 2010.
8. Yang, L., G. Orecchini, G. Shaker, H. Lee, and M. M. Tentzeris, "Battery-free RFID-enabled wireless sensors," *IEEE MTT-S International Microwave Symposium Digest (MTT)*, Vol. 75, No. 51, 1528–1531, Jul. 2010.
9. Balachandran, M. D., S. Shrestha, M. Agarwal, Y. Lvov, and K. Varahramyan, "SnO_2 capacitive sensor integrated with microstrip patch antenna for passive wireless detection of ethylene gas," *Electronics Letters*, Vol. 2, No. 7, 464–466, Mar. 2008.
10. Yoon, H., J. Xie, J. K. Abraham, V. K. Varadan, and P. B. Ruffin, "Passive wireless sensors using electrical transition of carbon nanotube junctions in polymer matrix," *Smart Materials and Structures*, Vol. 15, No. 1, Oct. 2006.
11. McGrath, M. P. and A. Pham, "Microwave vertically aligned carbon nanotube array sensors for ammonia detection," *IEEE Sensors*, Vol. 33, No. 5, 1–4, Mar. 2006.
12. Ren, X. and X. Gong, "A wireless sensing technique using passive microwave resonators," *IEEE Antennas and Propagation Society International Symposium, AP-S*, Vol. 6, No. 9, 1–4, Sep. 2008.
13. Ong, K. G., K. Zeng, and C. A. Grimes, "A wireless, passive

carbon nanotube-based gas sensor," *IEEE Sensors Journal*, Vol. 2, No. 2, 82–88, Apr. 2002.

14. Lupan, O., G. Chai, and L. Chow, "Novel hydrogen gas sensor based on single ZnO nanorod," *Microelectronic Engineering*, Vol. 85, No. 11, 2220–2225, Nov. 2008.
15. Kim, Y. S., S. C. Ha, K. Kim, H. Yang, S. Y. Choi, Y. T. Kim, J. T. Park, C. H. Lee, J. Choi, J. Paek, and K. Lee, "Room-temperature semiconductor gas sensor based on nonstoichiometric tungsten oxide nanorod film," *Appl. Phys. Lett.*, Vol. 86, No. 21, 1–3, Apr. 2005.
16. Wang, J. X., X. W. Sun, Y. Yang, H. Huang, Y. C. Lee, O. K. Tan, and L. Vayssieres, "Hydrothermally grown oriented ZnO nanorod arrays for gas sensing applications," *Nanotechnology Journal*, Vol. 17, No. 19, 1–10, Aug. 2006.
17. Tentzeris, M. M., "Inkjet-printed paper-based RFID and nanotechnology-based ultrasensitive sensors: The "green" ultimate solution for an ever improving life quality and safety?" *IEEE Radio and Wireless Symposium (RWS)*, Vol. 3, No. 56, 120–123, Mar. 2010.
18. Dragoman, M., A. Muller, D. Neculoiu, G. Konstantinidis, K. Grenier, D. Dubuc, L. Bary, R. Plana, H. Hartnagel, E. Fourn, and E. Flahaut, "Carbon nanotubes-based microwave and millimeter wave sensors," *European Microwave Conference*, Vol. 45, No. 89, 16–19, Dec. 2007.
19. Thai, T. T., A. Haque, G. R. De. Jean, and M. M. Tentzeris, "A novel ultrasensitive gas detector system based on carbon nanotube mixtures and antenna radiation variation," *IEEE Ant. & Prop. Society Int. Symp., AP-S*, Vol. 33, No. 42, 1–4, Sep. 2008.
20. Abdul Aziz, N. H., A. J. Alias, A. T. Hashim, R. Mustafa, S. S. Sarnin, N. A. Wahab, and W. N. W. Muhamad, "Smart integrated sensors in real time monitoring critical parameters in tissue culture growth room of oil palm," *Fifth International Conference on MEMS, NANO, and Smart Systems (ICMENS)*, Vol. 33, No. 2, 229–233, Jun. 2010.
21. Karabacak, T., J. S. DeLuca, D. Ye, P. I. Wang, G. C. Wang, and T. M. Lu, "Texture evolution during shadowing growth of isolated Ru columns," *J. Appl. Phys.*, Vol. 99, No. 064304, Apr. 2006.
22. Computer Simulation Technology/ Microwave Studio CST MWS, 2010, http://www.cst.com.
23. Silveirinha, M. G. and N. Engheta, "Sampling and squeezing electromagnetic waves through subwavelength ultranarrow regions or openings," PACS No. 78.66.Sq, 52.40.Db, 52.40.Fd, 42.70.Qs.